Icarus 198 (2008) 27–36

Contents lists available at ScienceDirect

Icarus

www.elsevier.com/locate/icarus

Lava flows at Arsia Mons, Mars: Insights from a graben imaged by HiRISE

Peter J. Mouginis-Mark [a,*], Scott K. Rowland [b]

[a] Hawaii Institute of Geophysics and Planetology, University of Hawaii, 1680 East-West Road, POST Room 504, Honolulu, HI 96822, USA
[b] Department Geology and Geophysics, University of Hawaii, Honolulu, HI 96822, USA

ARTICLE INFO

Article history:
Received 25 March 2008
Revised 23 June 2008
Available online 6 August 2008

Keywords:
Mars
Mars, surface
Volcanism

ABSTRACT

HiRISE has imaged a graben wall on the western flank of Arsia Mons volcano, Mars. This graben is $\sim 3 \times 16$ km in plan-view size and is oriented almost perpendicular to the general volcano slope. We have identified 1318 individual sub-horizontal layers, which we interpret to be lava flows, in the 885 m high, nearly vertical, eastern wall of this graben. The average and median outcrop widths of each layer are 149 and 85 m, respectively. No layers extend >1.72 km across the width of the section, arguing against these being either areally-extensive ash or paleo-glacial deposits, which has implications for the reoccurrence interval of glacial events and/or the long-term magma production rate of the volcano. Measurements ($N = 118$) made at a 100-m spacing across the width of the section reveal that there are, on average, 17.3 layers at each location. This implies an average layer thickness of $\sim$51 m. Locally, however, as many as 7 layers can be counted within a 70 m-high part of the section, implying, if these layers are indeed lava flows, that Arsia Mons occasionally erupted flows that were only $\sim$10 m thick.

1. Introduction

It has been difficult to the determine the long-term magma production rates, or even the typical volume of lava erupted per event, of martian volcanoes due to the problem of resolving either detailed flow stratigraphy or the relative ages of adjacent individual lava flows (Hartmann and Berman, 2000). Numerous surficial lava flows have been mapped on the Tharsis and Elysium volcanoes (Mouginis-Mark and Tatsumura-Yoshioka, 1998; Baloga et al., 2003; Bleacher et al., 2007; Garry et al., 2007), so that the widths, lengths and thicknesses of these flows can be used to estimate the total volume of each flow. However, these surface flows provide only a snap-shot of the most recent activity of a volcano, which might or might not be representative of earlier eruptive phases. A vertical section through a volcano (coupled with spatial information provided by the dimensions of lava flows) would avoid this limitation, because it would enable long-term trends in the eruptive sequence of a volcano to be studied (Mouginis-Mark and Rowland, 2001; McEwen et al., 2007). A vertical section would also provide an opportunity to study the erosional characteristics and spatial extent of eruptive units, perhaps allowing for differentiation between spatially-extensive ash deposits produced by major explosive eruptions (Mouginis-Mark, 2002), lava flows, or non-volcanic units such as glacial moraines, debris flows, or eolian deposits (Shean et al., 2007). However, with the exception of the walls of the summit calderas (Mouginis-Mark and Rowland, 2001), it is rare to see vertical sections of martian volcanoes.

The High Resolution Imaging Science Experiment (HiRISE) camera (McEwen et al., 2007) onboard the Mars Reconnaissance Orbiter provides the first opportunity to investigate the rare places where the stratigraphy of the top kilometer or more of Mars may be investigated at sub-meter spatial resolution at locations such as the walls of graben, canyons, and impact craters. A morphologically fresh graben on the western middle flanks of the volcano Arsia Mons was imaged at a resolution of 25 cm/pixel by HiRISE under lighting conditions that allow almost the entire near-vertical eastern wall to be investigated (frame PSP_004412_1715). The graben is centered at 8.57° S, 236.37° E, which is $\sim$105 km west of the summit caldera (Figs. 1 and 2). The graben is up to $\sim$3.1 km wide (WNW-ESE) and $\sim$16.4 km long (NNE-SSW). Its eastern rim is at an elevation of $\sim$6600 m and the western rim is at $\sim$6375 m. The graben is located at the boundary to what we interpret to be the summit lavas of Arsia Mons and the flank lavas (Fig. 1b). Knobby fan facies and smooth fan facies to the west of the graben are interpreted by Shean et al. (2007) to be glacial deposits. The graben tapers at both ends, merging to the north with two semi-circular collapse pits. Southwest of the southern end of the graben is a line of shallow collapse pits. A line connecting the collapse pits at the ends of the graben has an azimuth of 15°, whereas the long axis of the graben has an azimuth of 9°. The graben is essentially tangential to the general topographic contours of the volcano, so that it should cut at a right angle any units emplaced in a down-slope direction.

* Corresponding author. Fax: +1 808 956 3188.
E-mail address: pmm@higp.hawaii.edu (P.J. Mouginis-Mark).

0019-1035/$ – see front matter
doi:10.1016/j.icarus.2008.06.015

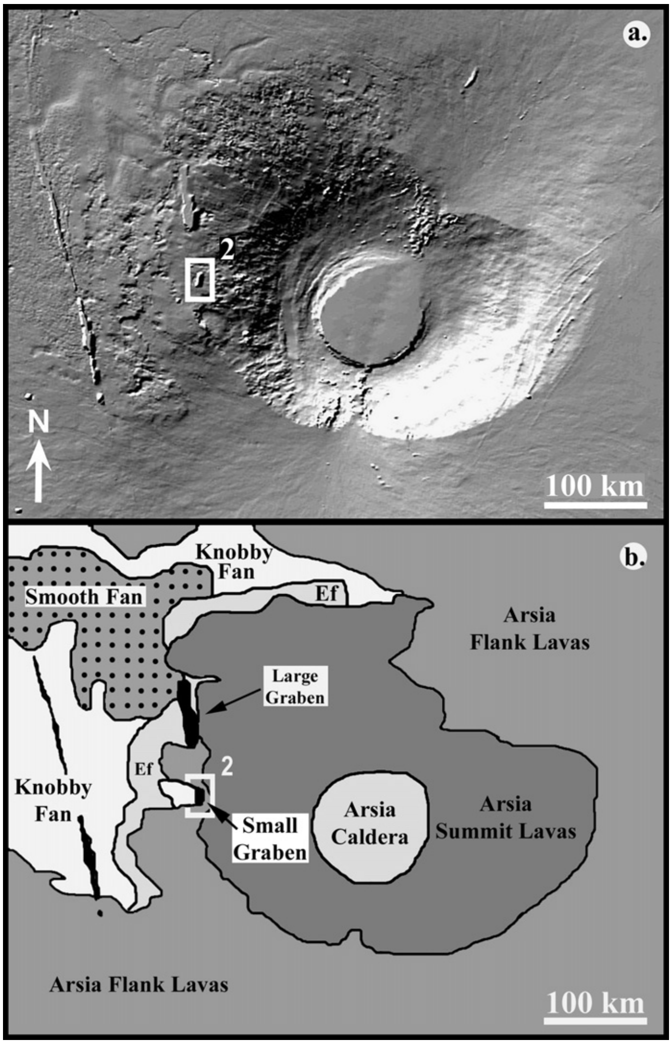

Fig. 1. (a) Location of the graben on the west flank of Arsia Mons volcano, with the white box indicating the location of Fig. 2. Base image is a shaded relief rendition of the MOLA 128th-degree data set with the illumination from the lower right. (b) Geologic sketch map of the region shown in Fig. 1a, partially adapted from Shean et al. (2007). They named the graben studied in this analysis the "small graben." "Ef" is a unit that is an eroded portion of the flank of Arsia Mons that does not appear to have either smooth or knobby fan facies, which Shean et al. (2007) interpret to be glacial deposits.

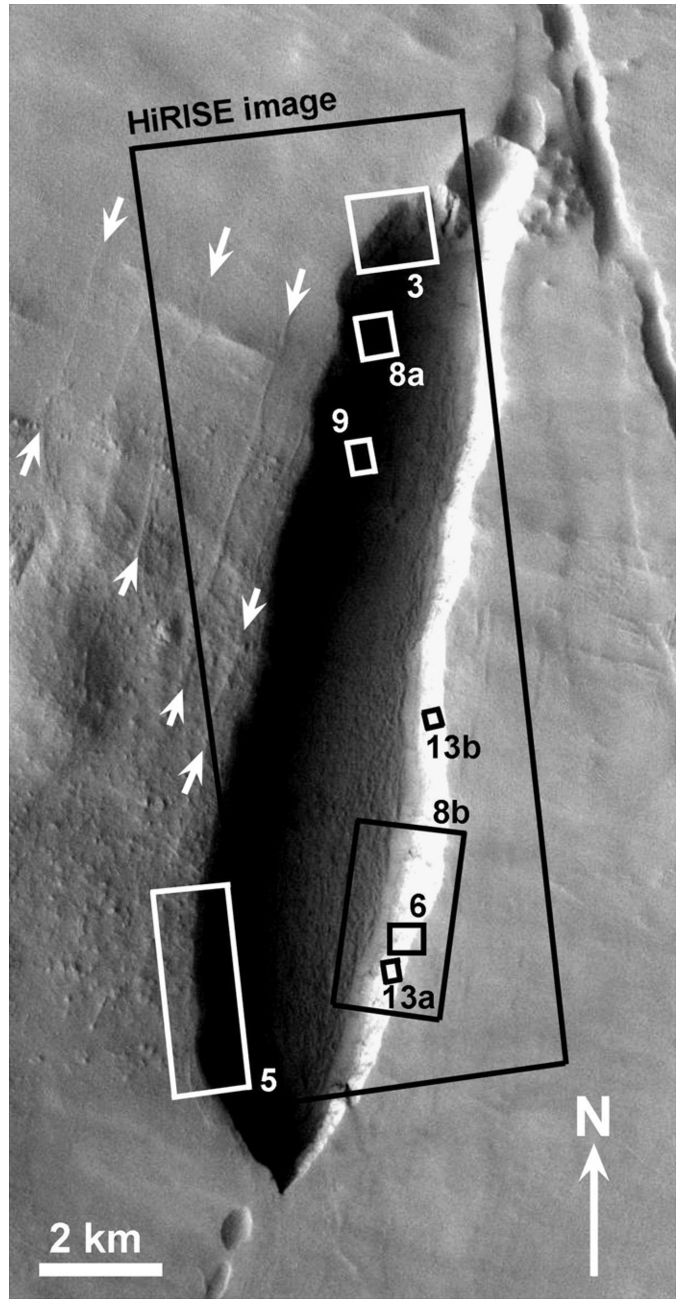

Fig. 2. Details of the graben studied here, which is centered at 8.57° S, 236.37° E. Large black rectangle denotes coverage by HiRISE frame PSP_004412_1715; small white and black rectangles show the location of Figs. 3, 5, 6, 8, 9 and 13. The drop moraine ridges on the western rim that were identified by Shean et al. (2007) are identified by the white arrows. Base image is THEMIS frame V15345002.

Fig. 3 illustrates the level of detail within the wall of the graben available in the HiRISE image. Numerous layers can be seen and, as we detail below, we interpret these layers to be lava flows.

2. Morphology of wall

Five different subdivisions of the vertical section of the graben can be identified along its length, shown schematically in Fig. 4: (1) a rim unit; (2) a main unit that displays numerous layers; (3) a secondary unit that does not outcrop along the entire length of the wall, but has thinner layers than the overlying unit; (4) a basal unit consisting of layers that are a morphologically different from those in the above two units; and (5) a unit consisting of the materials on the floor of the graben. There is also high albedo material on the walls themselves. These five main units are now described.

An image from the Mars Orbiter Camera (MOC) (Fig. 5) reveals that the upper few tens of meters of the graben wall have a more gradual slope, suggestive of preferential erosion of the rim unit, perhaps because it consists of less competent material than the main unit below. Layering is observable within this top-most unit. The top of the rim unit comprises the volcano surface outside the graben, and it is morphologically bland, although at the meter-scale there are examples of eolian dunes on both the eastern and western rims. Shean et al. (2007) identified several ridges west of the graben rim. These ridges (Fig. 2) are approximately parallel to the contours of the volcano and appear to be associated with lobate deposits on the flanks of Arsia Mons. Shean et al. (2007) have interpreted both these lobate deposits and the ridges as drop moraines from recent glacial events on Arsia Mons.

In our discussion of the main unit of the graben, we focus our attention on the eastern wall, which, along its entire length, is morphologically very similar to the segment of the wall illus-

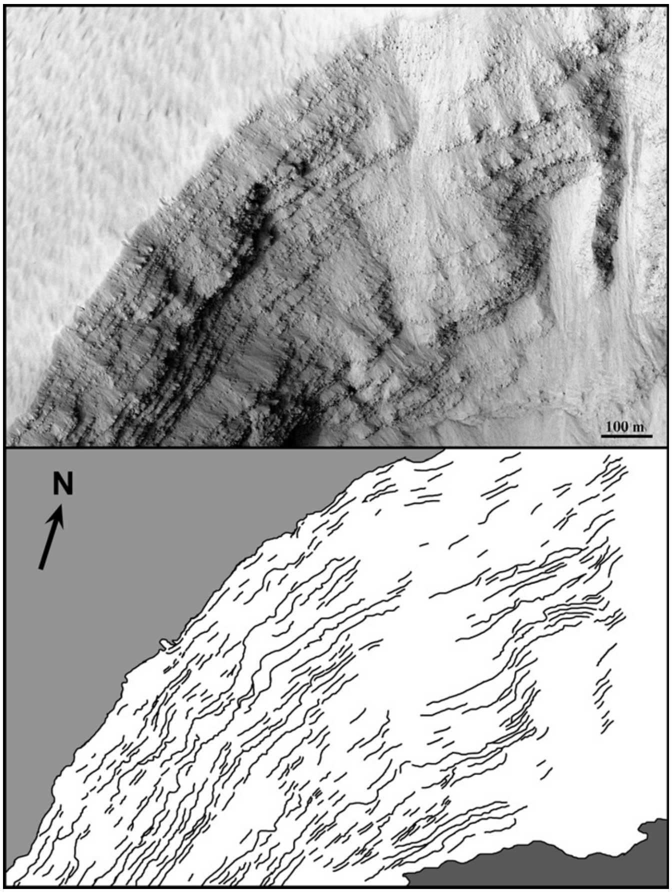

Fig. 3. Top: Segment of HiRISE image showing the cliff at the northernmost part of the graben. The rim is at the top of this image. See Fig. 2 for location. Bottom: Interpretative sketch of the HiRISE image showing the layers that are interpreted here to be individual lava flow units. Part of HiRISE frame PSP_004412_1715.

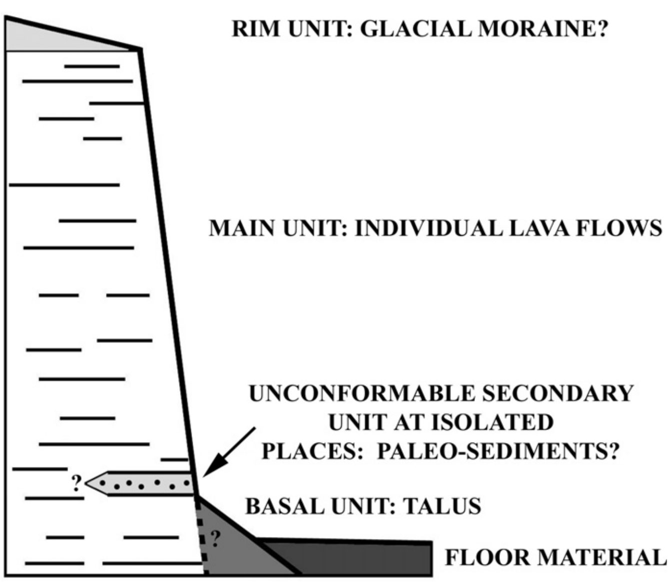

Fig. 4. Schematic sketch of the section of the eastern graben wall.

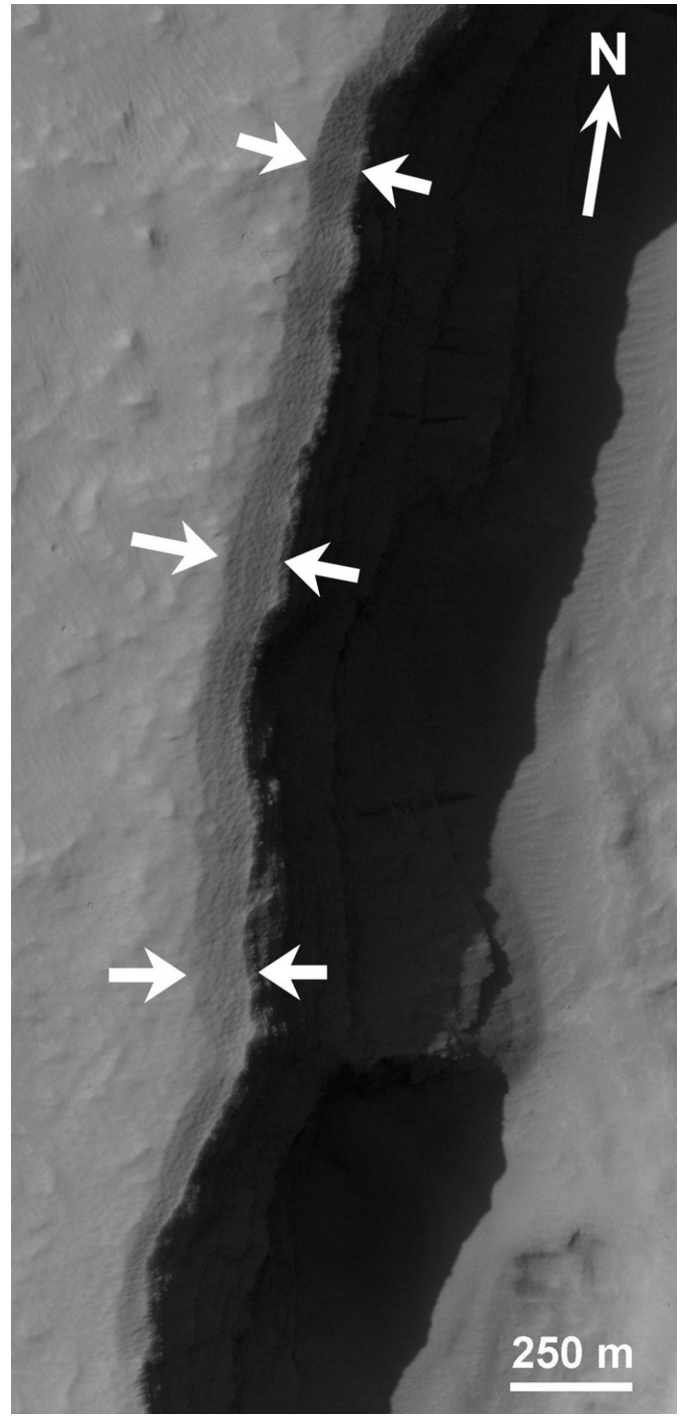

Fig. 5. Under different lighting conditions from those under which the HiRISE image was obtained, the shallower slope of the topmost unit (between arrows) on the western rim can be easily identified in MOC data. Several resistant "layers" can be seen in the shallow-dipping unit, suggesting that it is not a single unit. Image resolution is 1.5 m/pixel. See Fig. 2 for location. Part of MOC image S0300087.

trated in Fig. 3. HiRISE provides coverage of a 12.5 km-wide section of this wall (Fig. 2), and here the lighting geometry and dynamic range of the image permit virtually the entire wall to be mapped. Throughout the whole sequence of layers (Fig. 6), there is high albedo, morphologically-bland, material that extends down-slope for more than a few tens of meters. Numerous layered craggy outcrops can be seen at almost all elevations in the section. Some layers appear to be more resistant to erosion than others, forming small benches ~15–20 m wide in a horizontal direction perpendicular to the face of the graben.

When considering the distribution of the layers within the wall, it is important to keep in mind several potential complications, which include: (1) The lighting geometry has caused the parts of the wall directly facing the Sun to saturate in the HiRISE image. (2) Talus covers parts of wall. (3) Insufficient spatial resolution in

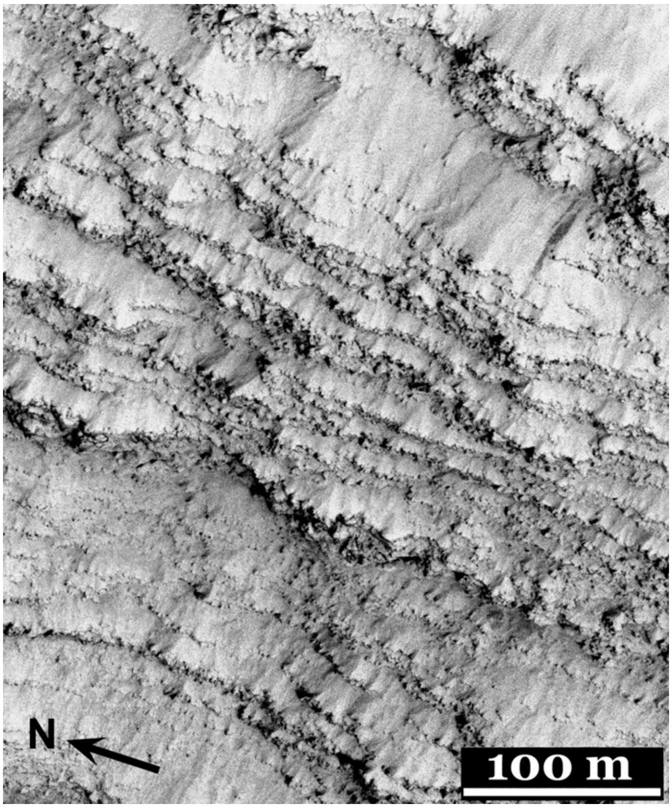

Fig. 6. Full resolution (25.6 cm/pixel) view of part of the eastern wall of the graben. The rim is seen at top right of the image. Note the blocky nature of many layers and, except for the layers at the top of the section, the lack of extensive amounts of talus. See Fig. 2 for location. Part of HiRISE frame PSP_004412_1715.

the image may lead to both the top and the bottom of a flow being mapped as individual units. (4) It may be very hard to differentiate two adjacent flows at the same stratigraphic level, and hence they may be counted as one. (5) The geometry of the wall, with several embayments and salients in the wall, tends to visually compress some units together in certain places, making individual flow units hard to identify. With these constraints on the identification of layers within the graben wall, we have mapped 1318 individual layers within the portion of the eastern wall imaged by HiRISE. Although individual layers can be traced for tens to hundreds of meters laterally, the exposures of bedrock are not continuous on a scale of 10 to 50 m; a certain level of image interpretation is therefore needed to define any discrete layer. Instead, each layer appears to consist of dark-toned knobs of intact rock separated by lighter-toned talus. The maximum horizontal width of any layer measured across the section is 1.72 km, and the average and median widths are 149 m and 85 m, respectively (Fig. 7). Such widths are very similar to the flow widths measured on Ascraeus Mons by Hiesinger et al. (2007). We have also counted the number of layers at 118 vertical profiles spaced 100 m apart. We find an average of 17.3 layers per profile (median value is 16), with a maximum of 30 layers and a minimum of 10 layers. No apparent pattern of a repeating sequence of layers, either vertically or horizontally, has been identified in the distribution of these layers.

In isolated places along the graben wall, we find a second set of layers at the base of the main unit (the "2nd unit" shown in Fig. 8). These layers lack the knobby texture of those in the main unit, and are unconformable with the layers above them. The HiRISE data show that the lowermost unit in the graben wall consists of layers that are quite different from those in the rim and main units (Fig. 8).

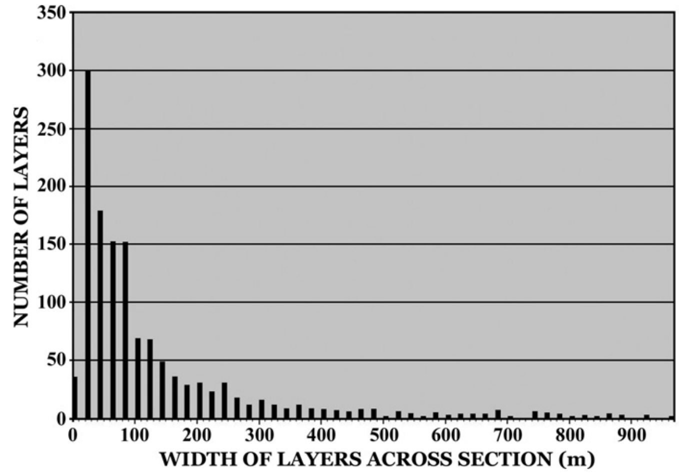

Fig. 7. Distribution of the lengths of layers identified in the eastern wall of the graben. Total width of section is ∼12.5 km. A total of 1318 individual layers have been identified.

The lowermost unit has a higher albedo than units higher up in the section. Unlike the rest of the graben wall, the basal unit also displays several examples of dark streaks, which are similar to the scars of recent landslides (cf. Gerstell et al., 2004; Schorghofer et al., 2007; Chuang et al., 2007). The boundary between this unit and the overlying layers is very distinct but the details of the stratigraphic relationship between these two units cannot be determined with great confidence. There are no lobes or landslides of talus that extend on to the floor of the graben.

Shean et al. (2007) hypothesized that there are ridges of glacial deposits on the floor of the graben. HiRISE data indicate that the floor of the graben has a number of low ridges running parallel to the long axis of the graben and is mantled (Fig. 9), but there are no unequivocal indications that the materials on the floor are glacial in origin. For example, we do not see kilometer-scale contiguous ridges comparable to those on the western rim of the graben that have been discussed by Shean et al. (2007). Exposures of possible bed-rock on the graben floor are mantled by layered deposits that have dune fields on their surfaces (Fig. 9).

3. Height of graben wall

A key factor in estimating the thickness of individual layers within the graben wall is the determination of the total wall height. Because of the orientation of the graben (almost north to south) and the uneven longitudinal spacing of the MOLA orbits, it is not possible to directly measure the wall height at many locations. There are sixteen MOLA orbits that cross the graben (Fig. 10). Two orbits (11,211 and 18,932) run almost north to south along the length of the graben, and an additional five orbits (13,707, 14,688, 15,015, 15,342, and 16,499) cross the southern graben floor. Six orbits (11,538, 12,965, 14,361, 18,586, 18,963, and 19,453) fall on the western rim, and three orbits (16,556, 17,235 and 19,422) fall on the eastern rim. These MOLA data allow several cross-sections to be constructed across the width of the graben.

We constructed four west-to-east cross-sections from the MOLA data (Figs. 10 and 11). To avoid bias from the possible erosion of the rim (i.e., the area arrowed in Fig. 5), we selected MOLA data points at least 200 m away from the rim in an attempt to measure the unaltered surface elevation. As a consequence of the slope of the volcano, the eastern side of the graben is ∼120 m higher than the western side. We extrapolated a straight line westward (and downward) from the two MOLA tracks east of the graben, and picked as the elevation of the eastern rim of the graben the elevation of this line where it intersected the eastern graben edge.

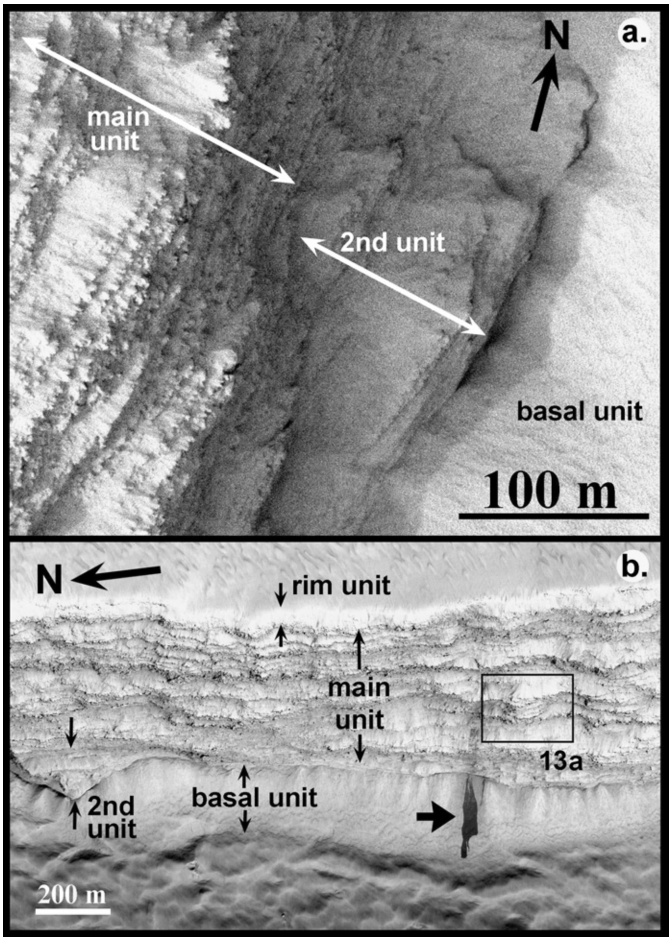

Fig. 8. Segments of the graben floor, showing the discontinuity between the layers within the upper part of the wall section, and a set of unconformable layers (the "2nd unit") at the base of the section. See Fig. 2 for location. (a) Western wall, showing the striking difference in the layer thickness and lack of blocks in the lower unit compared with the layers above it. (b) Eastern side of the graben floor, showing the unconformity of the lowermost layers. Note also that this segment of the graben wall displays numerous dark landslide scars (arrowed), suggesting that this unit is more friable than the overlying layers. Box outlines the part of the wall shown in Fig. 13b. Parts of HiRISE image PSP_004412_1715.

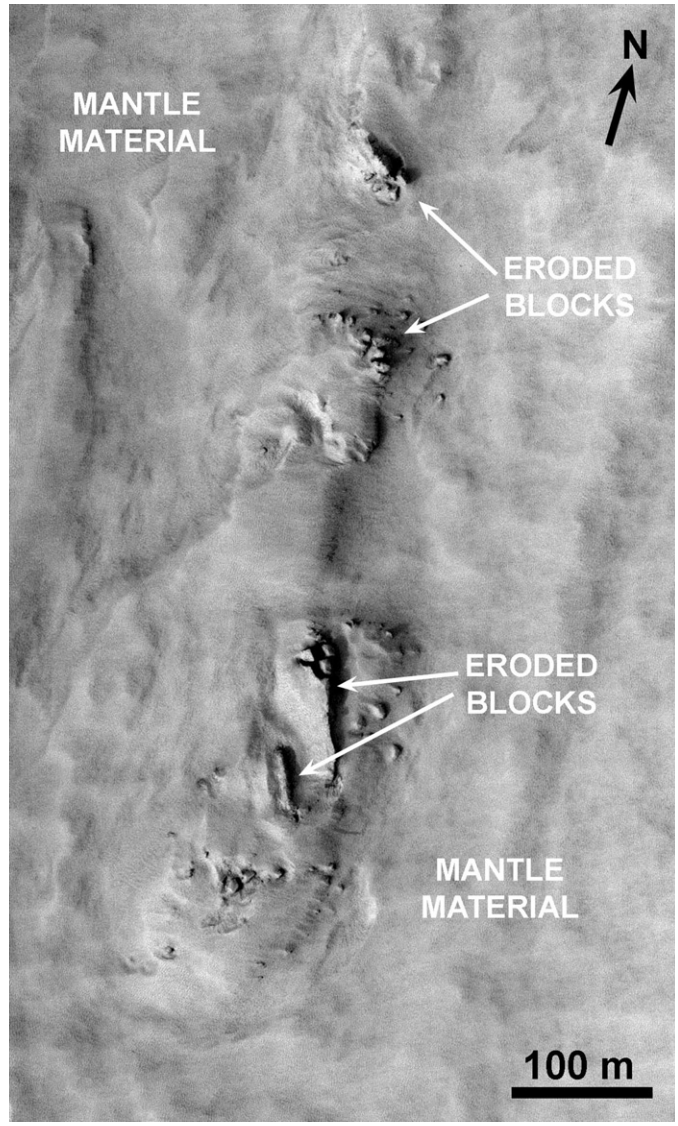

Fig. 9. Part of the floor of the graben. Note the remnants of (what we interpret to be) eroded bedrock on the floor, and the mantle of material that partially buries these blocks. See Fig. 2 for location. Part of HiRISE frame PSP_004412_1715.

We visually identified the eastern edge of the graben in THEMIS image V15345002. In order to obtain an accurate measurement of the thickness of the main unit, it was also necessary to determine the elevation of the top of the talus unit. MOLA orbit 11211 (identified in Fig. 10) allows us to estimate the thickness of this basal unit (Fig. 12). The elevation rises from the floor of the graben (elevation 5535 m) to 5684 m, and then drops to an elevation of 5648 m, defining a moat that is determined by a single MOLA shot. This moat is visible in the HiRISE image as a shallow depression along much of the base of the graben wall. We take the elevation of the floor of this moat to be the top of the talus unit and the base of the main unit; the elevation difference between the moat and the graben floor (113 m) is therefore the estimated thickness of the basal layer.

Using extrapolated rim elevations, and a constant basal unit thickness of 113 m, gives four estimates of the thickness of the main unit (Fig. 10): 881, 879, 887, and 892 m; an average of 885 m. We note that the use of the raw MOLA data, rather than an interpolated MOLA digital elevation model (DEM), is critical for the determination of the elevation of the graben floor. Shean et al. (2007) used the 128th degree MOLA DEM and inferred that the floor slopes to the south (their Fig. 10c). However, MOLA orbit 11211 shows that the floor is lowest (at an elevation of 5400 m) near the northern end of the graben. An issue that cannot be resolved with the available topographic data is the apparent near-constant elevation of the basal layers. MOLA data are of insufficient spatial density (particularly for the northern part of the graben floor) to determine if this base elevation is indeed constant, so we await the collection of a second HiRISE image to allow a stereo-derived digital elevation model (DEM) to be constructed, so that the dip of the basal units can be determined.

4. Interpretation of layers

The graben wall of Arsia Mons provides a remarkable view of a small part of the three-dimensional structure of a large shield volcano on Mars. Potentially the section provides information not only about the style of volcanism (effusive vs explosive eruptions, and high vs low discharge rate lava flows), but also the internal structure of the volcano and the potential re-occurrence of glacial events comparable to those documented by Shean et al. (2007). Taking the average height of the section to be 885 m, and the observation that within any one of our 118 vertical profiles there can be 10 to 30 layers, implies an average layer thickness between 88

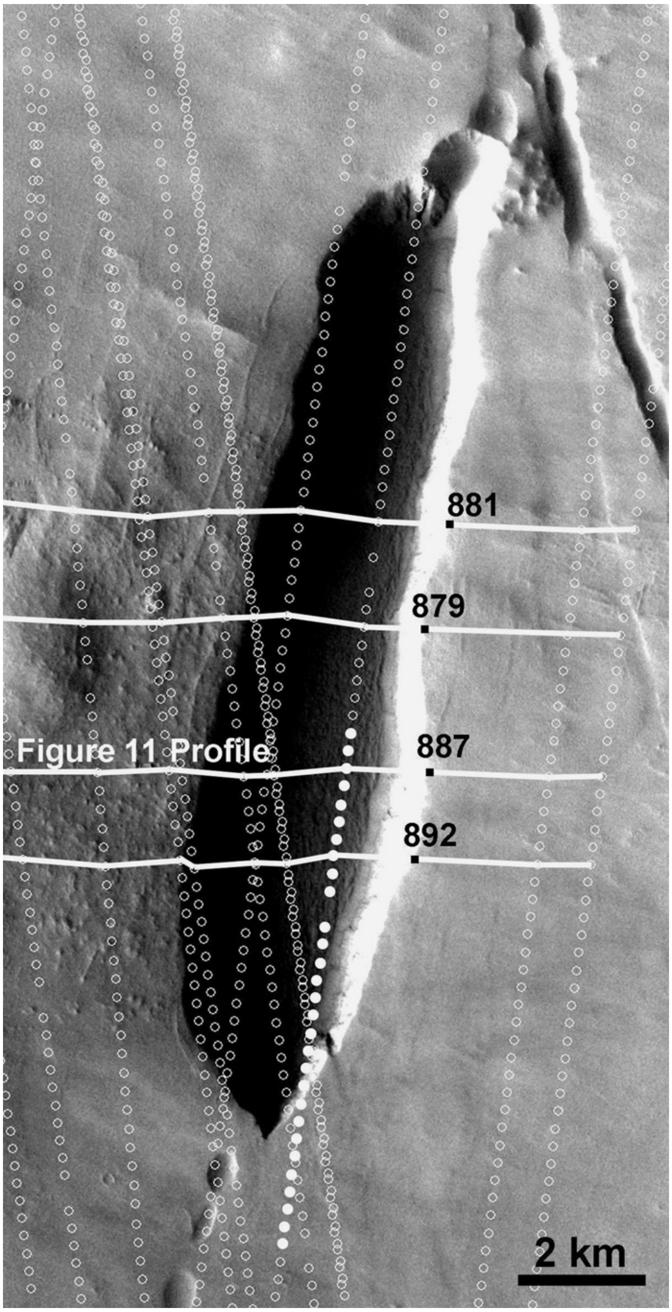

Fig. 10. Distribution of MOLA topographic data (open white circles) for the graben. The four horizontal white lines mark the locations of the cross-graben profiles that have been measured using multiple MOLA orbits (see Fig. 11). The small black squares show the derived heights of the east rim, which exclude the contribution from the basal layers (see Fig. 8). The solid white circles mark the location of a segment of MOLA profile 11211 used to investigate the thickness of the basal layer (see Fig. 12). Base image is THEMIS frame V15345002.

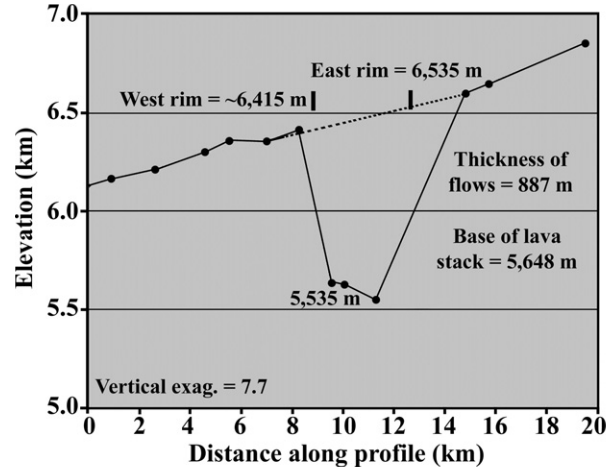

Fig. 11. One of the four west-to-east profiles across the graben using multiple MOLA orbits. Three additional profiles (not shown) were also constructed. MOLA points are solid circles. Extrapolating from the image (the two vertical lines labeled west and east rim) to get the actual location of the east rim, we derive 6535 m for its elevation. Given the elevation of the floor of the graben as 5535 m, and a thickness of 113 m for the basal layer (Fig. 12), this implies that the eastern wall is ∼887 m high, including the basal unit.

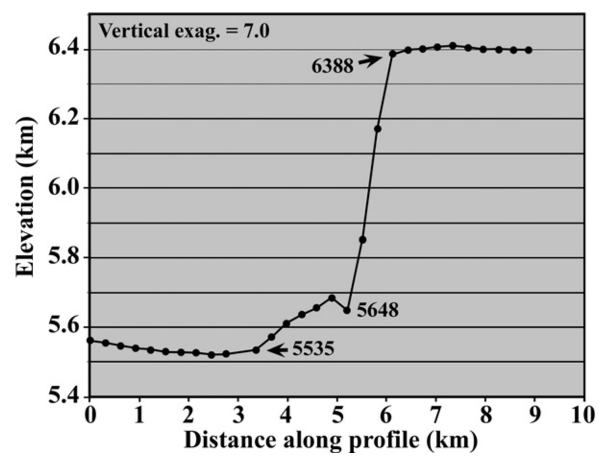

Fig. 12. MOLA profile 11211 allows the height of the bench at the base of the graben wall to be determined. There is a distinct break in slope at the southern end of the graben floor that gives a bench height of ∼113 m. Note that the height is taken at the "moat," or low point, right next to the wall of the graben.

and 30 m. Extreme cases of very thin layers (Fig. 13) also can be found, with a set of seven layers (Fig. 13a) having a total thickness of ∼70 m, or ∼10 m per flow. A key issue is, therefore, the interpretation of the layers.

Inspection of a 1 m/pixel resolution Ikonos satellite image and field data for an eroded section of the Koolau volcano in Hawaii (Fig. 14) reveals a remarkable similarity to the layers in the Arsia Mons graben. The layers seen in the section of the Koolau volcano at Makapuu Point are all lava flows, with a typical thickness of ∼1 to 2 m for compound pahoehoe flows and 3 to 5 m for aa flows. There are no dikes in this sequence of Hawaiian flows, nor are there any channelized flows preserved in section, so that it is not possible to test if HiRISE images could be used to identify comparable features on Mars. The fact that Arsia Mons and the Koolau volcano are both shield volcanoes lead us to believe that the layers in the Arsia Mons graben are lava flows. Indeed, the weathering characteristics of the layers appear to be the same at both locations, with the massive cores of aa flows forming steep slopes, and talus being present on the tops of individual layers as well as there being accumulations of talus at the foot of the sections. Alternative interpretations for the layers, such as pyroclastic flow or fall deposits, are unlikely because of the narrow width of the Arsia Mons layers. The Arsia Mons layers are also unlikely to be lahars, partly because of the narrow width and also because there appears to have been little incision into pre-existing layers. Air-fall ash deposits comparable to the ones proposed by Mouginis-Mark (2002) are discounted because of the lack of spatial continuity and the knobby texture of the layers. Because these alternative interpretations all seem to be less likely than lava flows, and the fact that the Makapuu flows closely resemble the Arsia Mons layers, we propose that the layers in the Arsia Mons graben are indeed lava

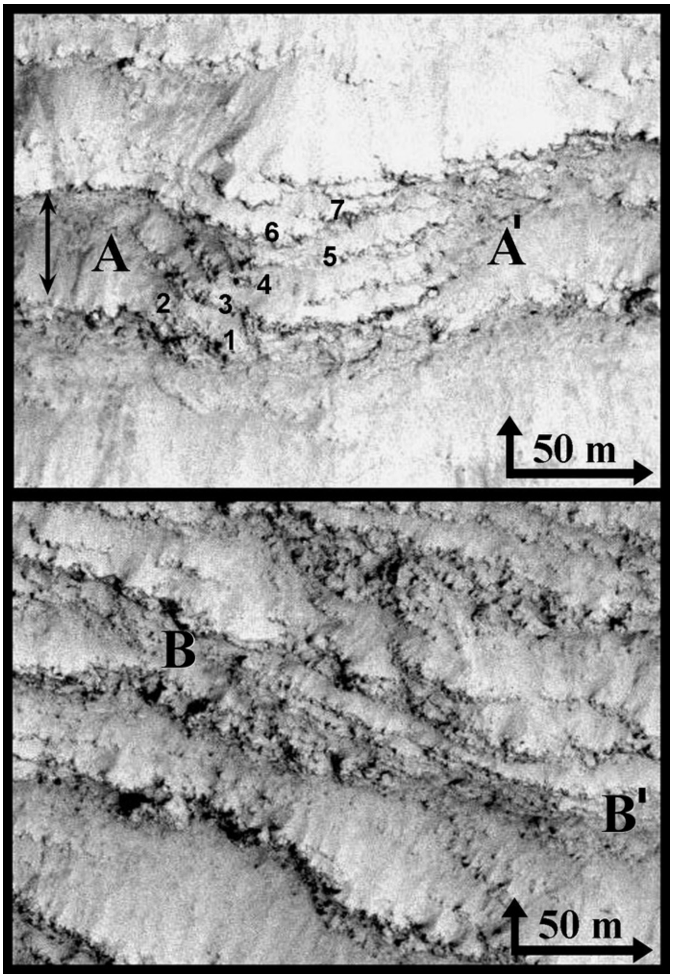

Fig. 13. Two segments of the eastern wall of the graben, showing spatial variability in the thickness and number of the layers; see Fig. 2 for locations. (a) is at the top of the graben section and (b) is near the bottom. Note the occurrence of numerous thin flows between A–A′ and B–B′. Seven individual layers are numbered in (a) at one location; to the north (left) a single layer is identified between the arrows. Both images are parts of HiRISE frame PSP_004412_1715. North is to the left in each image. Note that because the cliff face is seen obliquely, the vertical scale is different from the horizontal scale.

flows. The high albedo unit at the base of the Arsia Mons graben is therefore most likely to be talus derived from the lava flows above.

It is also instructive to compare the Arsia Mons lava flows with layers that may also be lava flows elsewhere on Mars. HiRISE has, for instance, imaged several parts of the Olympus Mons escarpment along the northern perimeter of the volcano where many tilted flow units can be identified (Fig. 15a). One of the side canyons within Ius Chasma, which is most likely an exposed segment of the upper part of the stratigraphic column of Syria Planum/Solis Planum (at 8.0° S, 274.4° E) also reveal multiple layers (Fig. 15b). At both Olympus Mons and Ius Chasma, the layering is more uniform than we observe at Arsia Mons and there is less evidence of the knobby morphology of the individual layers compared to, for example, the layers shown in Fig. 6.

5. Discussion

We can place the Arsia Mons graben in the context of other vertical sections that we can see on martian volcanoes. For example, there are several calderas that are more than 1 km deep (e.g., the Olympus Mons caldera is ∼3.2 km deep and that of Pavonis Mons is ∼4.8 km deep; Plescia, 2004). No detailed studies of HiRISE data of these caldera walls have been conducted to date, but our preliminary inspection of the available images confirms our earlier interpretations (Mouginis-Mark and Rowland, 2001; Mouginis-Mark and Christensen, 2005; Mouginis-Mark et al., 2007) that the flow units within the caldera walls are more laterally extensive than those in the Arsia Mons graben studied here. We also note that the Arsia Mons flows appear to be less spatially continuous than terrestrial examples such as the flood basalts seen on Earth at the Columbia River, the Karoo in southern Africa, or the Deccan of India (Francis, 1993, his Figs. 3.3 and 3.4) so that they were not erupted as high-volume lavas.

With the exception of fissure-fed flows erupted east of the volcano Jovis Tholus, which may be only 4–6 m thick (Mouginis-Mark and Christensen, 2005), all lava flows previously studied on Mars are >40 m thick (Mouginis-Mark and Tatsumura-Yoshioka, 1998; Baloga et al., 2003; Bleacher et al., 2007; Garry et al., 2007) and are thus more likely to be aa flows. The thin (∼10 m) flow units identified in Fig. 12 offer the intriguing possibility that some flows from Arsia Mons could be pahoehoe. Typically, pahoehoe flows on Earth are thinner that aa flows (Self et al., 1998); although locally, inflated pahoehoe flows have been identified in Hawaii (Walker, 1991), and flow units akin to pahoehoe within the flood basalts of Washington (USA) and the Deccan (India) can be greater than 20 m thick (Keszthelyi and Self, 1998; Sheth, 2006). It is not clear if these thinner flows on Arsia Mons are pahoehoe or aa, but the potential recognition of pahoehoe flow could have importance for martian volcanism because extensive pahoehoe lava is only erupted at a low effusion rate (Rowland and Walker, 1990).

There is no systematic difference between the top and the bottom of the lava stack, which suggests that there was no major shift in the style or volume of individual eruptions during the time period that is recorded here. The graben wall also enables us to address the long-term occurrence of explosive volcanism on Mars during the time period in which the layers exposed in the wall were emplaced on this part of Arsia Mons. Any pyroclastic fall or density current (ignimbrite) deposits that originated from the volcano would most likely outcrop in layers many kilometers in width (e.g., Wilson and Head, 1994) and be of constant thickness if exposed in a wall such as the one studied here that is approximately radial to the volcano summit. Our study has not identified any horizontally-extensive morphologically-uniform layers that might be outcrops of buried pyroclasts. Previously, Edgett (1997) and Mouginis-Mark (2002) have both speculated that Arsia Mons may have experienced explosive eruptions based upon the existence of bland layers seen, respectively to the west of the volcano and near the summit, as well as the unusually high abundance of fine material within the Tharsis region. We see no supporting evidence for such ash deposits at this range of ∼105 km from the rim of the caldera, at least during the time period over which the layers within the graben wall were emplaced, bringing into question the origin of the extensive deposits of fine materials within the Tharsis region (Edgett, 1997; Hynek et al., 2003).

For a similar reason, the lack of laterally extensive layers exposed in the wall of the graben is relevant to recent discussions of the paleo-climate of Mars, and specifically the origin of materials immediately west of the graben rim that have been proposed to be glacial drop-moraines (Shean et al., 2007). These moraines have been linked to climate excursions on Mars due to obliquity changes in the recent past (Costard et al., 2002; Marchant and Head, 2007; Kreslavsky et al., 2008). Although we do not know the time period over which the sequence of flows exposed in the graben wall was formed, it seems highly unlikely that all of these flows could have been erupted within an obliquity cycle of a few million years. If one were to assume that Arsia Mons formed over a time period of ∼2 billion years, and the ∼900 m graben wall represents ∼ 14.5%

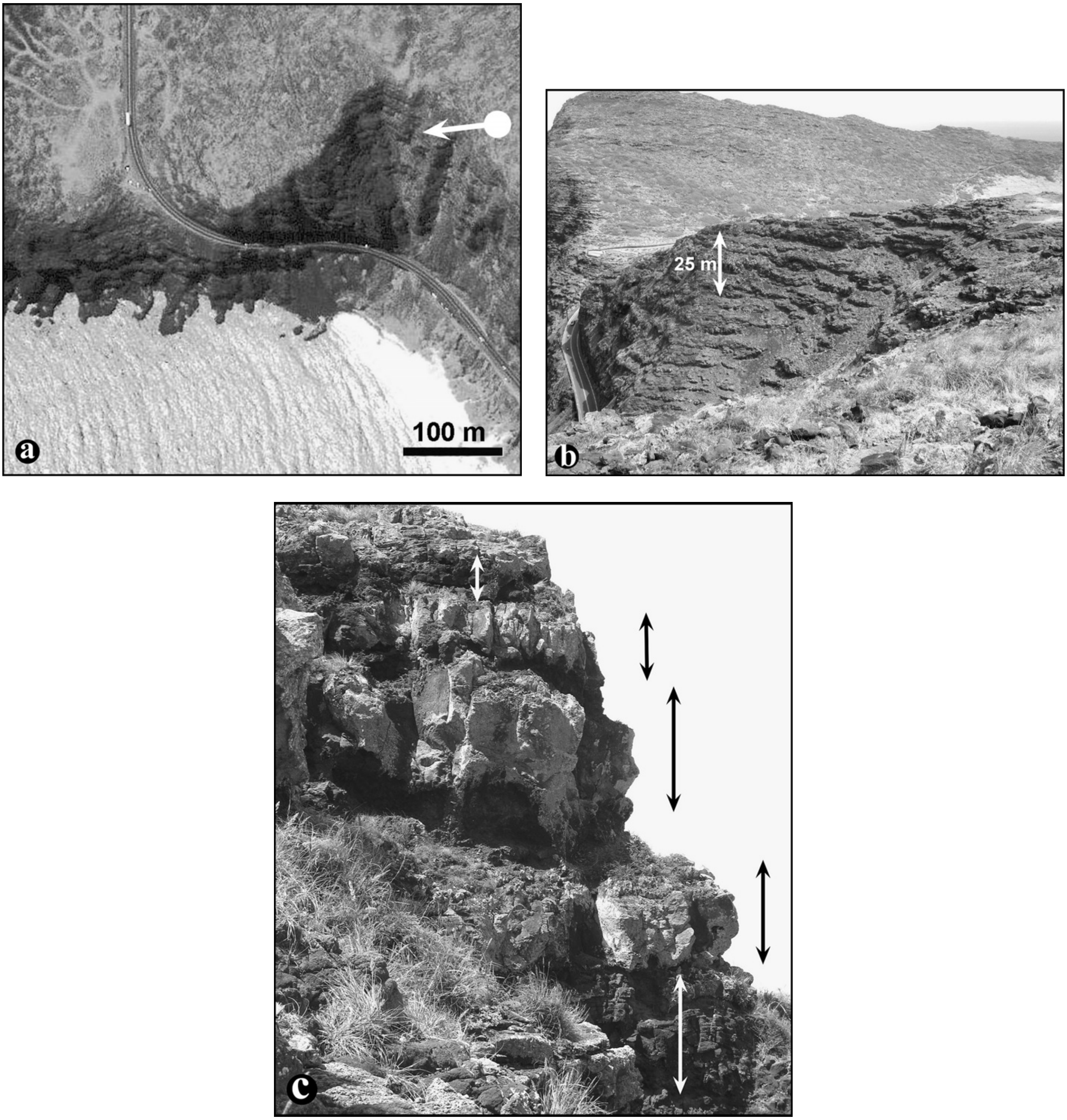

Fig. 14. (a) Ikonos satellite image (1 m/pixel resolution) of S.E. Oahu, Hawaii, showing an eroded section of the cliff face at Makapuu Point. The ocean is at the bottom of the image. Layering comparable to that seen within the Arsia Mons graben can be seen along the cliff. The white arrow marks the approximate location (and azimuth) from which the photo in (b) was taken. (b) Ground view looking approximately east towards Makapuu Point. Note the 25 m scale bar (derived from measurements made along the cliff rim), and the road at far left of this image, which is also visible in (a). (c) Detailed view of the layering at Makapuu Point. The individual lava flows seen here are ~3 to 5 m thick. The three most prominent, thick, layers (denoted by black arrows) are all aa lava flows, and the top and bottom layers (denoted by white arrows) are pahoehoe lava flows.

of the total height of the volcano at this location above the MOLA datum, then a uniform magma production rate would imply that the flows exposed in the graben wall would take ~290 M years to form. Given an age estimate of ~35–115 million years for the fill on the graben floor (Shean et al., 2007), one would expect to see 8 to 2.5 layers of moraines within the graben wall. Alternatively, if Arsia Mons took 3 billion years to form, the 900 m-high wall would form in 435 million years, and so should show evidence of ~12 to 4 glacial episodes.

We see no evidence for buried glacial layers in the graben wall, and so there is an inconsistency between proposed fluctuations in climate (e.g., Schorghofer, 2007) and plausible magma production rates for Arsia Mons. However, because the long-term magma production rate of any volcano on Mars is difficult to determine

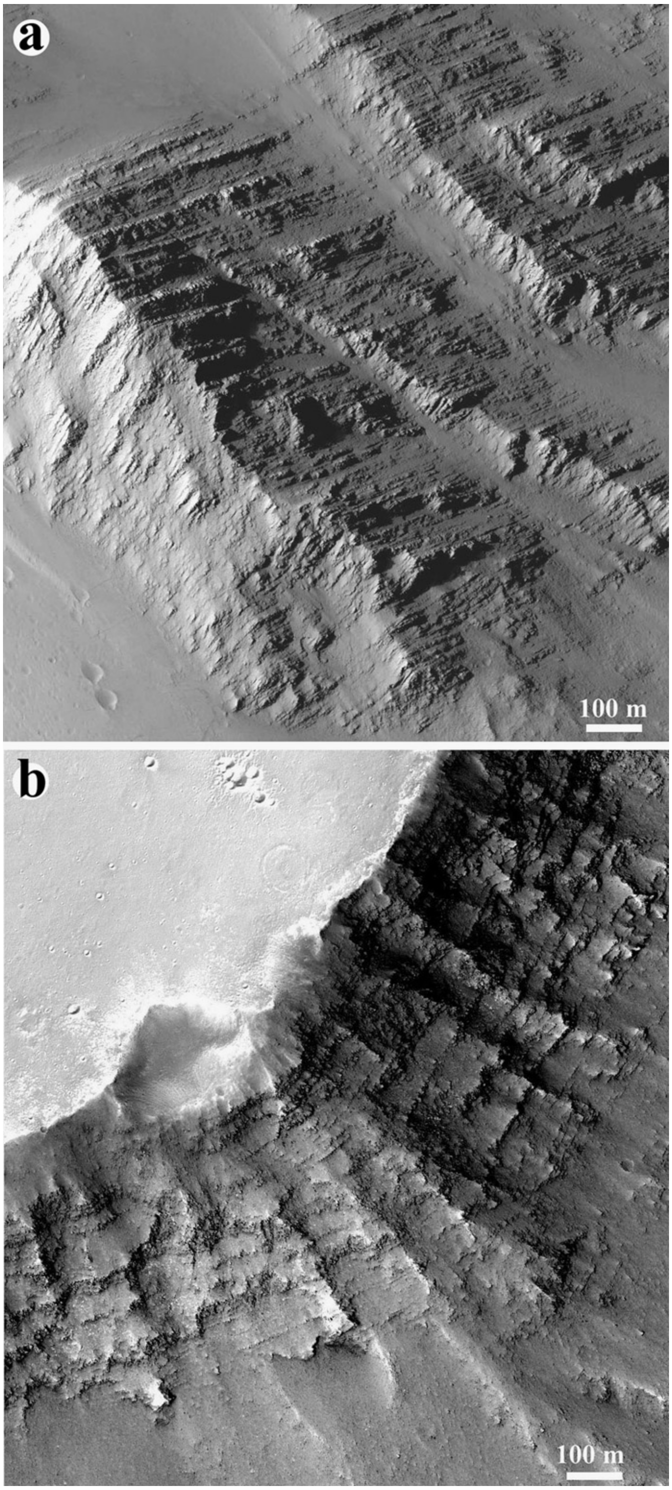

Fig. 15. (a) Tilted layers within the northern portion of the Olympus Mons escarpment. Note the very uniform flow thickness and horizontal continuity of the flows compared to the layers seen in Fig. 6. Part of HiRISE image PSP-007946_2035, centered at 23.3° N, 223.5° E. (b) Layers within the wall of a canyon close to Ius Chasma (at 8.0° S, 274.4° E) may be lava flows associated with volcanism within Syria Planum or Solis Planum. Note the absence of the knobby texture to the edges of these layers compared to the layers illustrated in Fig. 6. Part of HiRISE frame PSP_005004_1720.

(Wilson et al., 2001), the converse situation may also need further consideration in the future; namely that because we see no glacial layers within the graben wall, then the entire wall section may have formed during one glacial cycle of only a few million years. This rate of construction of the flanks of Arsia Mons would imply a much more prolific period of volcanism than can be implied by the formation of separate calderas at some of the Tharsis volcanoes. Wilson et al. (2001) deduced that there must have been repose periods of a few tens of million years between major eruptive episodes at Olympus Mons and Ascraeus Mons in order for one magma chamber to freeze prior to the on-set of the next episode of activity. Although Arsia Mons has only one very large caldera (and thus there is no physical evidence to suggest long-term breaks in the activity of the volcano), the lack of climate-related deposits in the graben cross section described in this paper would suggest that the magma production rates assumed for the volcano might be significantly too low. Future studies of the climate excursions of Mars in the recent geologic past (e.g., Schorghofer, 2007) should therefore consider this lack of evidence for earlier glacial events if the surficial deposits identified by Shean et al. (2007) are indeed drop moraines, as this interpretation has a critical role in trying to unravel the magma production rate of Arsia Mons.

Other observations made of the graben wall also provide useful information insights into the structure of Arsia Mons. In the graben, there are only a few cross-cutting features that could be dikes or faults, although we do see evidence for off-sets that may be oblique faults in the graben wall. This is consistent with the NE-SW structural trend of Arsia Mons (Crumpler and Aubele, 1978) because dikes would be expected to parallel this structural trend (Fiske and Jackson, 1972). Dikes would thereby be unlikely to intersect a roughly N–S graben on the west flank of the volcano. It is possible that some of the floor units are eolian mantle deposits, although we have not found any features typical of the eolian dunes that Bridges et al. (2007) have demonstrated can be seen at HiRISE resolution. These mantle deposits could be lake sediments or glacial till (Shean et al., 2007). We hypothesize that the moat identified in Fig. 12 may have been produced by strong along-graben-face winds impeding deposition at the base of the wall.

The HiRISE image studied here provides insight into the three-dimensional structure of a martian volcano. Whereas the relatively fresh appearance of the graben wall may be quite unusual, we can envision other locations where similar additional information may be obtained. The basal escarpment of Olympus Mons, deep pit craters at the middle elevations of Ascraeus, Pavonis and Arsia Montes, and the flanks of Tharsis Tholus (where flank collapse has exposed interior units; Plescia, 2003) offer particularly fruitful areas to be investigated in the future. If these parts of the volcanoes prove also to be relatively well-preserved, it should be possible not only to compare the typical activity as a function of time at one location, but also to determine if all of the volcanoes produced flows of comparable thickness and spatial extent during the past. We eagerly await additional HiRISE images to test these ideas.

Acknowledgments

We thank Alfred McEwen and the HiRISE Team for collecting the data that inspired this study, and for making the data available rapidly through their public web site http://hirise.lpl.arizona.edu/. This work was supported in part by NASA Grant NNG05GQ54G to PMM. We thank Harold Garbeil for producing the software that is used for merging the MOLA ground tracks with the THEMIS VIS images. Lionel Wilson provided helpful comments on an earlier draft of the text. Constructive formal reviews were provided by Larry Crumpler and Jacob Bleacher. This is HIGP Publication No. 1671 and SOEST Contribution No. 7535.

References

Baloga, S.M., Mouginis-Mark, P.J., Glaze, L.S., 2003. Rheology of a long lava flow at Pavonis Mons, Mars. J. Geophys. Res. 108 (E7), doi:10.1029/2002JE001981.

Bleacher, J.E., Greeley, R., Williams, D.A., Cave, S.R., Neukum, G., 2007. Trends in effusive style at the Tharsis Montes, Mars, and implications for the development of the Tharsis Province. J. Geophys. Res. 112 (E09), doi:10.1029/2006JE002873.

Bridges, N.T., Geissler, P.E., McEwen, A.S., Thomson, B.J., Chuang, F.C., Herkenhoff, K.E., Keszthelyi, L.P., Martinez-Alonso, S., 2007. Windy Mars: A dynamic planet as seen by the HiRISE camera. Geophys. Res. Lett. 34, doi:10.1029/2007/2007GL031445. L23205.

Chuang, F.C., Beyer, R.A., McEwen, A.S., Thompson, B.J., 2007. HiRISE observations of slope streaks on Mars. Geophys. Res. Lett. 34, doi:10.1029/2007GL031111. L20204.

Costard, F., Forget, F., Magnold, N., Peulvast, J.-P., 2002. Formation of recent martian debris flows by melting of near-surface ground ice at high obliquity. Science 295, 110–113.

Crumpler, L.S., Aubele, J.C., 1978. Structural evolution of Arsia Mons, Pavonis Mons and Ascraeus Mons: Tharsis region of Mars. Icarus 34, 496–511.

Edgett, K.S., 1997. Aeolian dunes as evidence for explosive volcanism in the Tharsis region of Mars. Icarus 130, 96–114.

Fiske, R.S., Jackson, E.D., 1972. Orientation and growth of Hawaiian volcanic rifts: The effect of regional structure and gravitational stress. Philos. Trans. R. Soc. London Ser. A 329, 299–326.

Francis, P., 1993. Volcanoes: A Planetary Perspective. Clarendon Press, Oxford, UK. 443 pp.

Garry, W.B., Zimbelman, J.R., Gregg, T.K.P., 2007. Morphology and emplacement of a long channeled lava flow near Ascraeus Mons volcano, Mars. J. Geophys. Res. 112, doi:10.1029/2006JE002803. E08007.

Gerstell, M.F., Aharonson, O., Schorghofer, N., 2004. A distinct class of avalanche scars on Mars. Icarus 168, 122–130.

Hartmann, W.K., Berman, D.C., 2000. Elysium Planitia lava flows: Crater count chronology and geological implications. J. Geophys. Res. 105 (E6), 15011–15026.

Hiesinger, H., Head, J.W., Neukum, G., 2007. Young lava flows on the eastern flank of Ascraeus Mons: Rheological properties derived from High Resolution Stereo Camera (HRSC) images and Mars Orbiter Laser Altimeter (MOLA) data. J. Geophys. Res. 112 (E05), doi:10.1029/2006JE002717.

Hynek, B.M., Phillips, R.J., Arvidson, R.E., 2003. Explosive volcanism in the Tharsis region: Global evidence in the martian geologic record. J. Geophys. Res. 108 (E09), doi:10.1029/2003JE002062.

Keszthelyi, L., Self, S., 1998. Some physical requirements for the emplacement of long basaltic flows. J. Geophys. Res. 103, 27447–27464.

Kreslavsky, M.A., Head, J.W., Marchant, D.R., 2008. Periods of active permafrost layer formation during the geologic history of Mars: Implications for circum-polar and mid-latitude surface processes. Planet. Space Sci. 56, 289–302.

Marchant, D.R., Head, J.W., 2007. Antarctic dry valleys: Microclimate zonation, variable geomorphic processes, and implications for assessing climate change on Mars. Icarus 192, 187–222.

McEwen, A.S., and 14 colleagues, 2007. Mars Reconnaissance Orbiter's High Resolution Imaging Science Experiment (HiRISE). J. Geophys. Res. 112, doi:10.1029/2005JE002605. E05S02.

Mouginis-Mark, P.J., 2002. Prodigious ash deposits near the summit of Arsia Mons volcano. Mars. Geophys. Res. Lett. 29, doi:10.1029/2002GL015296.

Mouginis-Mark, P.J., Christensen, P.R., 2005. New observations of volcanic features on Mars from the THEMIS instrument. J. Geophys. Res. 110 (E8), doi:10.1029/2005JE002421.

Mouginis-Mark, P.J., Rowland, S.K., 2001. The geomorphology of planetary calderas. Geomorphology 37, 201–223.

Mouginis-Mark, P.J., Tatsumura-Yoshioka, M., 1998. The long lava flows of Elysium Planitia, Mars. J. Geophys. Res. 103 (B11), 19389–19400.

Mouginis-Mark, P.J., Harris, A.J.L., Rowland, S.K., 2007. Terrestrial analogs to the calderas of the Tharsis volcanoes of Mars. In: Chapman, M. (Ed.), Environments on Earth: Clues to the Geology of Mars. Cambridge University Press, New York, pp. 71–94.

Plescia, J.B., 2003. Tharsis Tholus: An unusual martian volcano. Icarus 165, 223–241.

Plescia, J.B., 2004. Morphometric properties of martian volcanoes. J. Geophys. Res. 109 (E03), doi:10.1029/2002JE002031.

Rowland, S.K., Walker, G.P.L., 1990. Pahoehoe and a'a in Hawaii: Volumetric flow rate controls the lava structure. Bull. Volcanol. 52, 615–628.

Schorghofer, N., 2007. Dynamics of ice ages on Mars. Nature 449, 192–194.

Schorghofer, N., Aharonson, O., Gerstell, M.F., Tatsumi, L., 2007. Three decades of slope streak activity on Mars. Icarus 191, 132–140.

Self, S., Keszthelyi, L., Thordarson, Th., 1998. The importance of pahoehoe. Annu. Rev. Earth Planet. Sci. 26, 81–110.

Sheth, H.C., 2006. The emplacement of pahoehoe lavas on Kilauea and in the Deccan Traps. J. Earth Syst. Sci. 115 (6), 615–629.

Shean, D.E., Head, J.W., Fastook, J.L., Marchant, D.R., 2007. Recent glaciation at high elevations on Arsia Mons, Mars: Implications for the formation and evolution of large tropical mountain glaciers. J. Geophys. Res. 112, doi:10.1029/2006JE002761. E03004.

Walker, G.P.L., 1991. Structure and origin by injection of lava under surface crust, of tumuli, "lava rises," "lava-rise pits," and "lava-inflation clefts" in Hawaii. Bull. Volcanol. 53, 546–558.

Wilson, L., Head, J.W., 1994. Mars: Review and analysis of volcanic eruption theory and relationships to observed landforms. Rev. Geophys. 32, 221–263.

Wilson, L., Scott, E., Head, J., 2001. Evidence for episodicity in the magma supply to the large Tharsis volcanoes. J. Geophys. Res. 106 (E1), 1423–1433.